

# Optical and photoelectric properties of Mn-doped ZnS thin film on a flexible indium-tin-oxide/polyethylene terephthalate substrate prepared by pulsed laser deposition

Byeongdae Choi,\* Hyunseok Shim, Bunyod Allabergenov, and Myoung-Jae Lee

*Division of Nano and Energy Convergence Research, Daegu Gyeongbuk Institute of Science and Technology (DGIST), 50-1 Sang-Ri, Hyeonpung-Myeon, Dalseong-Gun, Daegu 711-873, South Korea*  
[bdchoi1@dgist.ac.kr](mailto:bdchoi1@dgist.ac.kr)

**Abstract:** Optical and photoelectric properties of Mn-doped ZnS thin films on indium–tin–oxide (ITO)/polyethylene terephthalate (PET) substrates by pulsed laser deposition (PLD) were investigated. The XRD patterns revealed that the thin film deposited at room temperature (RT) had a wurtzite phase, which changed to a sphalerite phase at a substrate temperature of approximately 100 °C. The transmittance of the films was approximately 87% in the visible range. The optical bandgap of the film deposited at RT was 3.29 eV, which increased to 3.361 eV with increasing substrate temperature to 200 °C. The photoluminescence (PL) intensity at 468 nm and the photocurrent by UV irradiation increased in proportion to the substrate temperature. The present results imply that Mn-doped ZnS films deposited on flexible PET substrates are useful for fabricating flexible optoelectronic devices such as flexible UV detectors.

©2016 Optical Society of America

**OCIS codes:** (310.0310) Thin films; (310.6860) Thin films, optical properties; (250.0250) Optoelectronics; (250.5230) Photoluminescence.

---

## References and links

1. S. Song, J. Jeong, S. H. Chung, S. M. Jeong, and B. Choi, "Electroluminescent devices with function of electro-optic shutter," *Opt. Express* **20**(19), 21074–21082 (2012).
2. S. Chung, S. Song, K. Yang, S. M. Jeong, and B. Choi, "Luminance enhancement of electroluminescent devices using highly dielectric UV-curable polymer and oxide nanoparticle composite," *Opt. Mater. Express* **4**(9), 1824–1832 (2014), doi:10.1364/OME.4.001824.
3. B. Farkas, T. Nyberg, and L. Nanai, "Flexible thin-film transistors on planarized parylene substrate with recessed individual backgates," *Solid-State Electron.* **94**, 11–14 (2014).
4. T. V. Prevenslik, "Acoustoluminescence and sonoluminescence," *J. Lumin.* **87–89**, 1210–1212 (2000).
5. J. J. Steele, A. C. van Popta, M. M. Hawkeye, J. C. Sit, and M. J. Brett, "Nanostructured gradient index optical filter for high-speed humidity sensing," *Sens. Actuators B Chem.* **120**(1), 213–219 (2006).
6. D. Chen, F. Huang, G. Ren, D. Li, M. Zheng, Y. Wang, and Z. Lin, "ZnS nano-architectures: photocatalysis, deactivation and regeneration," *Nanoscale* **2**(10), 2062–2064 (2010).
7. G. Boutaud, W. M. Cranton, D. C. Koutsogeorgis, R. M. Ranson, C. Tsakonas, and C. B. Thomas, "Growth optimisation of ZnS:Mn thin film phosphors for high intensity miniature electroluminescent displays," *Adv. Technol.* **165**, 202–206 (2009).
8. H. Haddad, A. Chelouche, D. Talantikite, H. Merzouk, F. Boudjouan, and D. Djouadi, "Effects of deposition time in chemically deposited ZnS films in acidic solution," *Thin Solid Films* **589**, 451–456 (2015).
9. W. S. Ni, Y. J. Lin, H. C. Chang, C. J. Liu, and L. R. Chen, "Luminescence behavior and compensation effect on the hole concentration in the sol-gel Zn<sub>1-x</sub>Cu<sub>x</sub>S<sub>y</sub> films with different compositions," *J. Lumin.* **168**, 241–244 (2015).
10. S. Ummartyotin and Y. Infahsaeng, "A comprehensive review on ZnS: From synthesis to an approach on solar cell," *Renew. Sustain. Energy Rev.* **55**, 17–24 (2016).
11. P. Chelvanathan, Y. Yusoff, F. Haque, M. Akhtaruzzaman, M. M. Alam, Z. A. Alothman, M. J. Rashid, K. Sopian, and N. Amin, "Growth and characterization of RF-sputtered ZnS thin film deposited at various substrate temperatures for photovoltaic application," *Appl. Surf. Sci.* **334**, 138–144 (2015).
12. A. I. Inamdar, S. Cho, Y. Jo, J. Kim, J. Han, S. M. Pawar, H. Woo, R. S. Kalubarme, C. J. Park, H. Kim, and H. Im, "Optical properties in Mn-doped ZnS thin films: Photoluminescence quenching," *Mater. Lett.* **163**, 126–129 (2016).

13. J. Cui, X. Zeng, M. Zhou, C. Hu, W. Zhang, and J. Lu, "Tunable blue and orange emissions of ZnS:Mn thin films deposited on GaN substrates by pulsed laser deposition," *J. Lumin.* **147**, 310–315 (2014).
14. S. C. Sharma, "A review of the electro-optical properties and their modification by radiation in polymer-dispersed liquid crystals and thin films containing CdSe/ZnS quantum dots," *Mater. Sci. Eng* **168**, 5–15 (2010).
15. A. C. Dhanya, K. V. Murali, K. C. Preetha, K. Deepa, A. J. Ragina, and T. L. Remadevi, "Effect of deposition time on optical and luminescence properties of ZnS thin films prepared by photo assisted chemical deposition technique," *Mater. Sci. Semicond. Process.* **16**(3), 955–962 (2013).
16. A. Ates, M. A. Yildirim, M. Kundakci, and A. Astam, "Annealing and light effect on optical and electrical properties of ZnS thin films grown with the SILAR method," *Mater. Sci. Semicond. Process.* **10**(6), 281–286 (2007).
17. S. Yano, R. Schroeder, H. Sakai, and B. Ullrich, "High-electric-field photocurrent in thin-film ZnS formed by pulsed-laser deposition," *Appl. Phys. Lett.* **82**(13), 2026–2028 (2003).
18. H. C. Ong and R. P. H. Chang, "Optical constants of wurtzite ZnS thin films determined by spectroscopic ellipsometry," *Appl. Phys. Lett.* **79**(22), 3612–3614 (2001).
19. J. J. Xu and J. F. Tang, "Optical properties of extremely thin films: studies using ATR techniques," *Appl. Opt.* **28**(14), 2925–2928 (1989).
20. M. McLaughlin, H. F. Sakeek, P. Maguire, W. G. Graham, J. Molloy, T. Morrow, S. Laverty, and J. Anderson, "Properties of ZnS thin films prepared by 248-nm pulsed laser deposition," *Appl. Phys. Lett.* **63**(14), 1865–1867 (1993).
21. B. Choi, H. Shim, and B. Allabergenov, "Red photoluminescence and blue-shift caused by phase transformation in multilayer films of titanium dioxide and zinc sulfide," *Opt. Mater. Express* **5**(10), 2156 (2015).

## 1. Introduction

II–IV semiconductors have recently attracted much attention as optoelectronic materials for the development of flexible devices such as digital signage and smart window films because they are fabricated by a cost-effective technique at low temperatures, which is especially important when using substrates made from organic materials [1–3]. ZnS is a wide bandgap compound semiconductor with high transmittance in the visible range, and thus it is useful in a wide range of applications, including displays, solar cells, sensors, and photocatalysts [4–10]. So far, a number of research groups have fabricated ZnS thin films using a variety of techniques and have investigated their electro-optical properties [11–20]. ZnS generally shows two stable phases: sphalerite [cubic (F43m)] and wurtzite [hexagonal (P63mc)]. The sphalerite phase is more stable than the wurtzite phase at low temperature below 1020 °C under the pressure of 1 bar. A study on multilayer films of ZnS/TiO<sub>2</sub>/ZnS reported that the phase transformation of ZnS from the sphalerite to the wurtzite structure was promoted at 600 °C in ambient conditions, and the film emitted photoluminescence (PL) in the red range [21]. By Mn ion doping, in addition to the emission from the near-band-edge (NBE) in the ultraviolet (UV) range, ZnS thin films emit visible light attributed to defects, including sulfur vacancies and Zn interstitials generated by the dopants [12]. Cui et al. reported that the blue emission shifted to orange by changing the deposition temperature in pulsed laser deposited Mn-doped ZnS films [13]. A detailed understanding of the thin-film growth and optical and photoelectrical properties of ZnS at low temperatures is necessary in order to control the quality of flexible devices. However, so far, few systematic studies on ZnS thin films deposited at low temperatures have been reported. In this work, we report on Mn-doped ZnS films prepared by pulsed laser deposition (PLD) onto indium–tin–oxide (ITO)/polyethylene terephthalate (PET) substrates at low temperatures. The results showed that the crystalline phase of the film changed at approximately 100 °C. The optical bandgap, the photocurrent caused by UV irradiation, and the emission intensity centered at 468 nm increased in proportion to the substrate temperature.

## 2. Experimental

The ITO/PET substrates were ultrasonically cleaned first with acetone and then with alcohol for 15 min before drying in air. After transferring the substrate to a holder block through the load-lock chamber, the PLD chamber was pumped to a pressure of  $2 \times 10^{-7}$  Torr prior to deposition. To promote stoichiometric reactions of the Mn-doped ZnS, Ar gas was flowed into the chamber at a rate of 30 sccm, and the working pressure was held at 200 mTorr during the deposition. To investigate the effects of the deposition temperature on crystal growth, we prepared Mn-doped ZnS thin films with thicknesses of 200 nm at RT, 100, 150, and 200 °C.

The KrF excimer laser (wavelength: 248 nm) was irradiated onto the 5 wt% Mn-doped ZnS target surfaces 5 cm above the substrate for 10 min at a repetition rate of 5 Hz to deposit the 200-nm-thick Mn-doped ZnS film. The PL properties were evaluated at RT (excitation wavelength: 300 nm) with a photospectrometer (JASCO FP-6500, light source: Xe lamp). The photocurrent caused by UV radiation was estimated by a homemade dark box equipped with a continuous-wave (CW) UV lamp (VL-4.LC, radiation wavelength: 365 nm, frequency: 50-60 Hz, and intensity:  $610 \mu\text{W}/\text{cm}^2$ ) and sourcemeter (Keithly-2400). The Ag metal (Sigma-Aldrich, 99.99%) strips for electrodes, with a space of 1 mm between them, were deposited onto the ZnS films using a shadow mask by thermal evaporation. The cables were fixed with silver paste (ELCOAT p-100, CANS, Japan) onto the Ag strips and directly connected to the sourcemeter to read the photocurrent. The crystal and surface structures of the films were measured with an X-ray diffractometer (Bruker, D2 PHASER, Cu  $K\alpha$ ,  $\lambda = 0.15406 \text{ nm}$ ) and atomic force microscopy (AFM, XE-100).

### 3. Results and discussion

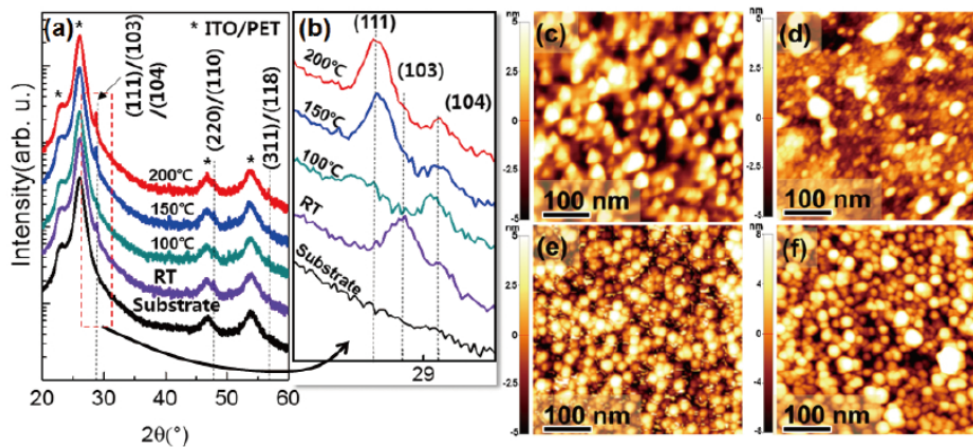


Fig. 1. Phase changes of the 5% Mn-doped ZnS thin films on ITO/PET substrates deposited by pulsed laser deposition. (a) XRD patterns at various substrate temperatures. (b) Magnification of the XRD patterns at small angle range. AFM images of the films at (c) RT, (d) 100 °C, (e) 150 °C, and (f) 200 °C.

Figure 1 shows the XRD patterns of the Mn-doped ZnS thin films deposited at various temperatures. The PET substrate coated with ITO shows four peaks having broad widths at  $23.1$ ,  $26.1$ ,  $46.7$ , and  $53.7^\circ$  [Fig. 1(a)]. The Mn-doped ZnS thin film deposited at RT shows four peaks of (103), (104), (110), and (118) caused by the wurtzite phase of ZnS. When the substrate temperature was increased to 100 °C, the (103) peak disappeared and a new broad peak with a small intensity at a smaller angle began to appear. The sequence of the peak change over the smaller angle range according to the substrate temperature is more clearly presented in Fig. 1(b). Increasing the substrate temperature to 150 °C led to enhancement of the peak, which was identified as (111), caused by the sphalerite phase. The peak was predominant for the film deposited at 200 °C. All samples showed a (104) peak, but the (103) peak drastically decreased at 100 °C, and the small, broad (111) peak caused by the sphalerite phase appeared. The sphalerite phase is more stable than the wurtzite phase at low temperatures under a pressure of 1 bar. In our previous work, we reported the paradoxical result that the wurtzite phase was deposited by PLD at room temperature but the sphalerite phase condensed at 500 °C because PLD is not an equilibrium process. The present result indicates that the phase change of wurtzite to sphalerite starts at approximately 100 °C. The surface mobility of the deposits increases with increasing substrate temperature, and the stable sphalerite (111) phase forms at 100 °C. The AFM surface images shown in Figs. 1(c)–

1(f) support this consideration. The film deposited at RT [Fig. 1(c)] has porous and rather large grains as compared to the film at 100 °C [Fig. 1(d)]. In general, the grain size of the thin film increases with increasing deposition temperature. However, in this study, the thin films deposited at 100 °C had the smallest grain size, which increased with increasing deposition temperature [Figs. 1(e), 1(f)]. This is considered to be because the nucleation and growth of the sphalerite phase evolved at approximately 100 °C. At the initial stage of the film growth, the energetic deposits explosively evaporated by pulsed laser could form a wurtzite phase that is stable at high-temperature regimes over 1020 °C on the substrate. Then, at substrate temperatures lower than 1020 °C, the deposits with the wurtzite phase preferentially reconstruct to the sphalerite phase because it is the stable phase of ZnS at low temperatures. To do this, the deposits have to overcome the energy barrier for the phase change. However, RT is not high enough to promote the phase change of the deposits, and the wurtzite phase preferentially grows at this temperature. The present results indicate that the sphalerite phase of ZnS starts to condense on the substrate at approximately 100 °C. These structural changes can induce variations in the electro-optical properties of ZnS. In order to investigate the variations in the emission centers, we measured the PL properties, and the resulting spectra are shown in Fig. 2. The thin films have emissions at 410, 468, and 557 nm. No predominant shifts in emission centers were observed by the phase change.

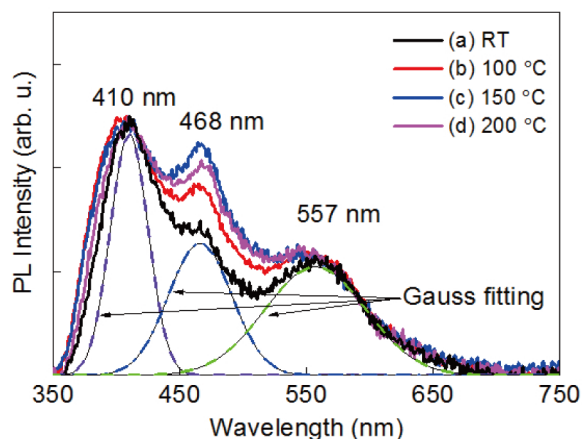


Fig. 2. Photoluminescence spectra of the 5% Mn-doped ZnS thin films on ITO/PET substrates by pulsed laser deposition at (a) RT, (b) 100 °C, (c) 150 °C, and (d) 200 °C.

The emissions at 410 and 557 nm are mainly attributed to Zn and sulfur vacancies, respectively [13]. The emission intensity centered at 468 nm, ascribed to Zn interstitials generated by Mn ion doping of ZnS, increased with increasing substrate temperature.

The transparency of the materials is an important optical property in terms of its applications. The Mn-doped ZnS films on ITO/PET substrate showed approximately 87% transmittance in the visible range (400–800 nm) regardless of the deposition temperature. As shown in Fig. 3(a), small fluctuations within the error range of  $\pm 5\%$  in the film transmittance were observed with increasing substrate temperature up to 200 °C [see inset in Fig. 3(a)].

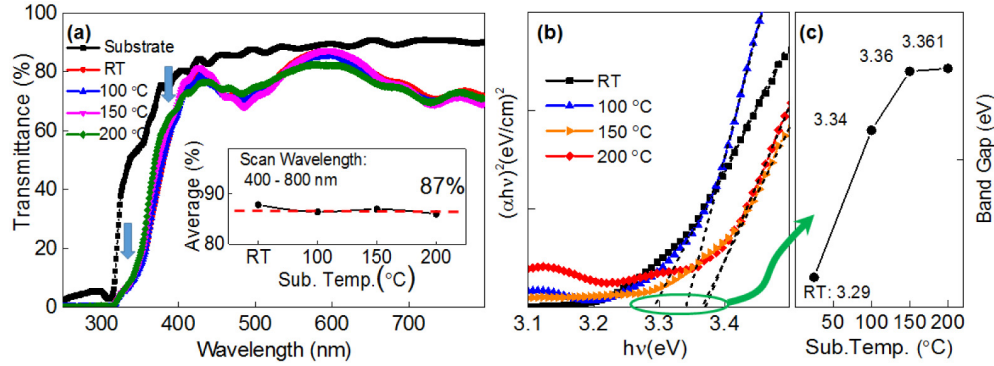


Fig. 3. Variation of the optical properties of the 5% Mn-doped ZnS thin films on ITO/PET substrates deposited at various temperatures by pulsed laser deposition: (a) transmittance, inset: average transmittance, (b) Tauc plot, and (c) optical bandgap

The transmittance depends on the film thickness, surface roughness, and light-scattering sites, including voids and defects, in the sample. The surface morphology revealed by AFM in Fig. 1 shows that the film deposited at RT has a loose packing structure, and its density increases with increasing temperature. The results mean that the transmittance in the visible range of the thin films deposited in this temperature range was not affected by the small changes in the film structure. In contrast, the transmittance in the UV range (320–370 nm), indicated by arrows in Fig. 3(a), drastically decreased as compared to the bare substrate. This is related to the optical absorption of the Mn-doped ZnS thin films. The optical bandgap of bulk ZnS changes from 3.54 to 3.8 eV according to its crystalline structure. The corresponding optical absorption edge of the wurtzite and sphalerite phases of ZnS are 350 and 326 nm, respectively. The Tauc plots in Fig. 3(b) show that the optical bandgaps of the Mn-doped ZnS thin films shift to higher values; the thin film deposited at RT has an optical bandgap of 3.29 eV, which increases to 3.361 eV with increasing substrate temperature as shown in Fig. 3(c).

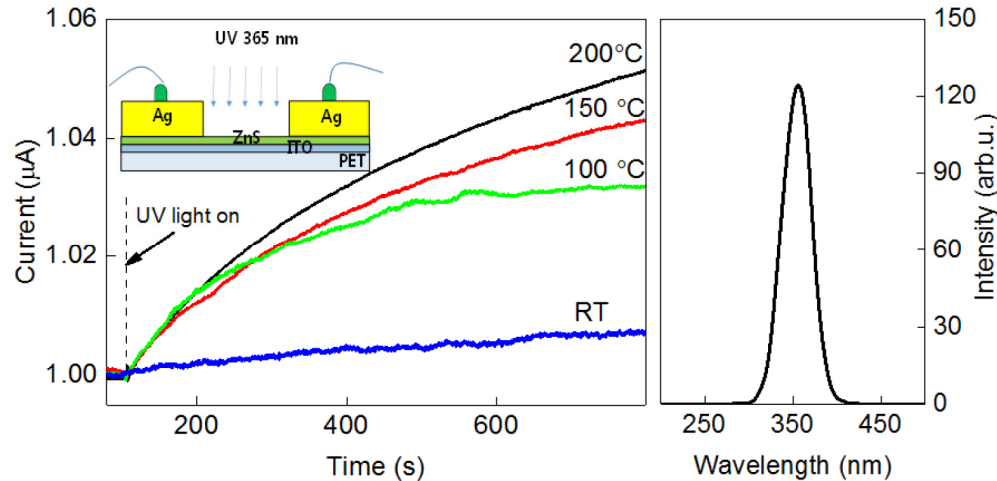


Fig. 4. (a) UV-photocurrent of the 5% Mn-doped ZnS thin films on ITO/PET substrates prepared at various temperatures and (b) spectrum of UV lamp.

These are small bandgap values as compared to those of the bulk ZnS, which means that the bandgap change in the films was not caused by the phase transition from the wurtzite to the sphalerite phase. The defects in the thin film, including vacancies and interstitials, cause the poor crystalline quality; as a result, the bandgap of the thin films could decrease.

Meanwhile, from the optical bandgap, the optical absorption edge of the thin film deposited at RT shifted to a longer wavelength of 383 nm, and it decreased to 375 nm upon increasing the deposition temperature to 200 °C. A careful examination of the plots shows that the optical bandgap of the higher-temperature sample is shifted to the shorter wavelength. The photocurrent measurement irradiated with 365 nm UV light shown in Fig. 4(a) reveals clear differences in the thin films according to the deposition temperature. The results indicate that Mn-doped ZnS thin films on PET substrates are useful for detecting UV light. The detailed configuration of the photocurrent measurement is shown in the inset of Fig. 4(a). The spectrum of the UV light used in this experiment is presented in Fig. 4(b). The photocurrent of the films increased slightly in the RT film shown in Fig. 4(a) after turning on the CW UV lamp that has the stabilization time of 50 ms to reach maximum CW-intensity. It drastically increased and depended on the substrate temperature in the films deposited at temperatures over 100 °C, as shown in Fig. 4(a). The photocurrent inversely depends on the defects because they provide traps for charge carriers. Defects in thin films such as pores or vacancies decrease with increasing substrate temperature; therefore, the photocurrent increases in proportion to the substrate temperature.

#### 4. Summary

In summary, the Mn-doped ZnS thin film exhibited wurtzite-to-sphalerite phase changes at a substrate temperature of approximately 100 °C. The PL intensity centered at 468 nm caused by Mn-ion doping increased with increasing substrate temperature. The transmittance of the film was approximately 87%, which fluctuated within an error range of 5% with deposition temperature. The optical band gap of 3.29 eV of the RT film increased to 3.361 eV due to the enhancement of crystalline quality with increasing substrate temperature. The photocurrent increased with increasing substrate temperature, which implies that the Mn-doped ZnS thin films on flexible PET substrate are useful for fabricating flexible optoelectronic devices such as flexible UV detectors.

#### Acknowledgments

This work was supported by the basic research program (16-NB-05) through the Daegu Gyeongbuk Institute of Science and Technology (DGIST), funded by the Ministry of Science, ICT, and future planning of Korea